Materials Science and Technology

Quantitative 3D characterization of Porous NiTi fabricated by Self High Temperature Synthesis (SHS) using X-ray micro-tomography. [Special Issue]

--Manuscript Draft--

Manuscript Number:	MST11558
Full Title:	Quantitative 3D characterization of Porous NiTi fabricated by Self High Temperature Synthesis (SHS) using X-ray micro-tomography. [Special Issue]
Article Type:	Research Paper
Keywords:	Porous NiTi; SHS; Micro-tomography; Bone implant
Corresponding Author:	Chiradeep Gupta, Ph.D Bhabha Atomic Research Centre Mumbai, INDIA
Corresponding Author Secondary Information:	
Corresponding Author's Institution:	Bhabha Atomic Research Centre
Corresponding Author's Secondary Institution:	
First Author:	Chiradeep Gupta, Ph.D
First Author Secondary Information:	
Order of Authors:	Chiradeep Gupta, Ph.D
	Elke van De Casteele, Ph.D
	Martine Wevers, Ph.D
	H Hoshino, Master
	M Kobayashi, Ph.D
	A Biswas, Ph.D
Order of Authors Secondary Information:	
Abstract:	A porous NiTi prepared by SHS for bone applications has been characterized by a commercially available laboratory X-ray micro-tomography instrument to reveal the structure of the internal porosity in 3D. The reconstructed slices tomography scan showed open porosity as well as micro-pores in the matrix. The 3D renderings revealed that the open porosity are highly interconnected structures and possesses a tortuous shape. Three dimensional quantitative estimates of the micro-pores in terms of their volume fraction, number density and size have been evaluated. Metrics based on skeletonized idealization of the complex architecture of interconnected pores that reflect its structural properties have been developed.
Suggested Reviewers:	
Additional Information:	
Question	**Response**
<b>Is your paper invited to be part of a SPECIAL ISSUE? Please type in 'YES' or 'NO' in the box below. If your answer is YES, please type in the title of your special issue and the name of the Guest Editor<b/>	Yes Cavitation studies in Materials : New Insights Guest Editor : Chiradeep Gupta

For Special issue in MST on "Cavitation ....

Quantitative 3D characterization of Porous NiTi fabricated by Self High Temperature Synthesis (SHS) using X-ray micro-tomography

C. Gupta[1], Elke van de Casteele[2], Martine Wevers[2], H. Hoshino[3], M. Kobayashi[3], A. Biswas[1]

1: Materials Group, Bhabha Atomic Research Centre, Mumbai 400085 India
2: Department of Materials Engineering, K. U. Leuven MTM, Kasteelpark, Avenberg 44 - bus 2450 BE 3001 Haverlee Belgium.
3: Department of Mechanical Engineering, Toyohashi University of Technology, Toyohashi 441-8150, Aichi Japan.

Abstract

A porous NiTi prepared by SHS for bone applications has been characterized by a commercially available laboratory X-ray micro-tomography instrument to reveal the structure of the internal porosity in 3D. The reconstructed slices tomography scan showed open porosity as well as micro-pores in the matrix. The 3D renderings revealed that the open porosity are highly interconnected structures and possesses a tortuous shape. Three dimensional quantitative estimates of the micro-pores in terms of their volume fraction, number density and size have been evaluated. Metrics based on skeletonized idealization of the complex architecture of interconnected pores that reflect its structural properties have been developed.

Introduction

The functional requirements of bone implants are quite complex[1]. A candidate bone implant material should be biocompatible containing a porous structure that has significant load bearing ability without undergoing permanent distortions at large strains[1,2]. In this regard the structural properties of animal and human bone classified as a porous ceramic material, are quite unique with Young Modulus in the range 10 – 30 GPa, and recoverable strain of about 2%[1,2]. Thus an ideal implant material combines load bearing and corrosion resistive properties with super-elasticity. The various classes of porous materials that have been investigated as bone implants are structural ceramics[3], polymeric[4] and metallic materials[5]. While ceramics are highly corrosion resistant and can withstand the loads imposed on the implant its inherent brittleness has been found to be a disadvantage[2]. Ductile porous polymeric materials on the other hand have poor load bearing properties as their Young Modulus values are low[2]. Thus porous metallic materials have been intensely investigated to tailor them for bone implant applications as they have not

only outstanding load bearing properties, as with bio-compatible materials such as Co- and Ti-based alloys but also possess superior fatigue and fracture resistance[6,7]. A key factor for tailoring these metallic materials is to introduce porosity in a manner that reduces both the modulus and permits the biological fixation of the implant by in-growth of the surrounding mineralized tissue[8-10]. This strategy to achieve implant stability is better than to use bone cements or screws for fixing it[1,2,11,12]. For this purpose many fabrication techniques have been devised that impart a spatial distribution of porosity in the materials that range from being random to being functionally graded[2,13-15]. Despite the fact that the porosity can be introduced in a controlled manner resulting in tailored bone implant architecture, the modulus mismatch between the surrounding bone/mineralized tissue and the metallic implants of Co- and Ti- alloys remains significantly high for the stress shielding effects to occur, that has been found to lead to bone re-sorption[2]. Thus the quest for implant material that matches the unique combination of properties of animal and human bone is an active interest of research.

The past decade has seen an interest in the use of porous Nitinol (NiTi: an equi-atomic alloy of Ni and Ti) as an implant material in maxilla-facial and orthopedic bone replacement surgeries[16-19]. It has many attractive properties suitable for implant material. Low modulus (only 1.5 to 2 times the modulus of bone as compared with 5-10 times in case of Co- or Ti- alloys), adequate load bearing capacity and bio-compatibility are some of the properties suitable to make this class of materials to be candidates for bone implants[20]. Further NiTi is a shape memory alloy (SMA) with super-elastic properties which provides a considerable edge amongst the porous metallic class of materials to mimic the novel structural properties of bone[21,22]. Since the first attempts to prepare NiTi using the SHS technique by Li and co-workers nearly ten years ago[23,24], active research has been focused on the developing alternatives to SHS processing (eg. CF-HIP), rendering pore surfaces to be bio-active to increase its bio-compatibility, optimizing the pore architectures and using ternary SMA alloys for bone implant applications[25]. In this regard a relatively scant description of the pore architecture in bone implants abounds the scientific literature. Considering the fact that porosity is an important functional requirement of bone implant its accurate characterisation is of utmost necessity[26]. This is best described in terms of 3D quantitative parameters as the shape, size, and morphology of pores can be completely described. The recent explosive growth in the application of micro-tomographic technique to characterize the internal damage in structural materials[27,28] and thereby provide new insights into

failure mechanisms in materials has not been applied in a significant manner to characterize the porosity in bone implants. In this paper a novel single phase porous NiTi fabricated by SHS technique using Plane Wave Propagation (PWP) mode has been subjected to micro-tomography characterization to quantitatively characterize the porosity in 3D emphasizing the morphology, connectivity and tortuosity of the open pores. The results have been discussed with regard to the possible influences that the porosity architecture has on the functional performance of the bone implant.

Experimental

The single phase porous NiTi (Ni51Ti49) has been prepared using PWP mode of SHS. The method reported earlier by Roy and Biswas[29,30] is briefly recapitulated here. Ni and de-hydrided Ti powder were dry mixed in nearly equi-atomic proportions in a tumbler ball mill and made into cylindrical porous green compact of 25 mm diameter and 100 mm length. SHS of NiTi enabled by an exothermic heat of reaction between Ni and Ti (~ 67 kJ/mol) was carried out on the green compacts under argon atmosphere. The reaction was started on the top of a compact by exploding a Kanthal A-1 spiral by passing large current through it. Once initiated, the exothermic reaction became self-sustaining and propagated through the compact in the form of a narrow luminous synthesis zone. Figure 1 shows the NiTi cylinder fabricated using the above technique. A small volume at the edge was cut of suitable dimension to be scanned by a commercial laboratory x-ray micro-tomography to characterize the porosity architecture. For the purpose of scanning a Skyscan 1172 micro-tomograph operating at 100 kV and 250µA was used that illuminated the sample of average cross-section 2.9 x 2.45 mm^2(measured from the center point of the sample). The length of sample scanned was 3.54 mm making the volume of the scan to be about 25 mm^3. The micro-focus X-ray source illuminated the sample with a cone beam geometry to generate projection images captured on a 2000 (H) x 1048(V) pixel CCD camera(pixel size 11.72µm) operated on 2x2 binning mode. During the scans sample was rotated for 180° in 0.4° increments with exposure time of 2.95s. The reconstruction was carried out using commercially available software from Skyscan implementing a modified feldkamp algorithm to provide the dataset in the form of 962 slice in the 16 bit Tiff image format. The reconstruction was carried out using an isotropic voxel size of 3.54µm. In order to reduce beam hardening Al+Cu filter was used as well as a software correction applied on the reconstructed dataset. A software correction

for ring artifacts available with Skyscan was also applied. Rendering of the dataset and its 3D visualization was carried out using VGStudioMax. A custom made software in Matlab was used to carry out quantitative analysis of the dataset in term of the new parameters of porosity characteristics.

Results and Discussion

Figure 2 shows the slice set corresponding to three distance levels below the top of the sample that was scanned in the tomograph machine. In each reconstructed slice set the matrix has been given a grey color in the 16 bit Tiff format. The porosity is represented as black areas in the slices. The background air is also represented as black. in order to demarcate the air from the porosities present in the matrix an yellow line highlights the sample borders in the reconstructed image slices. Therefore the black areas inside the yellow borders are porosities (fig 2a). The porosity present in the single phase NiTi prepared by explosive SHS that can be distinguished into three types. These are : open porosity, closed porosity and micro-pores distributed within the matrix. These have been indicated in the respective slices of the figure. It may be noted that the presence of micro-pores have not been reported in previous SHS works used to fabricate porous NiTi. The nature of the open porosity was seen to be quite complex. These open porosity not only are individually distributed but also have interconnections between them. Figure 2b shows a montage illustrating the interconnectivity nature of the porosity. The slice at a depth of 145µm shows two open porosity labeled as OP1 and OP2. At a further depth of 303µm the two open pore channels OP1 and OP2 are connected together. At 400µm the pore channels are separated out. This illustrates the typical feature of the porosity architecture that consists of interconnected pores.

The complete architecture is more clearly visualized in the 3D renderings carried out on the reconstructed dataset. Figure 3 shows the 3D visualizations of the matrix, open porosity and the micro-pores distributed in the matrix viewed from different perspective angles (0°, 90°, and 180°). The matrix is depicted as gray scale where large open areas can be seen especially in the perspective angle of 180° . These are the open porosity regions which have been segmented out as yellow in the figure 3. The morphology of the open porosity is now clearly visible in the scanned volume showing its complex shape and connectivity. The micro-pore present in the

matrix has also been segmented out and is depicted as red in last column corresponding to each of the perspective views. Because of the non-destructive nature of the technique it has been possible to not only to quantify the porosity content but also visualize in 3D the morphological nature of the open porosity. It is however instructive to compare the overall porosity results with the green density determined from Archimedes measurements. The tomography scans yielding reconstructed slice dataset, followed by the segmentation of the matrix and porosity on the basis of the attenuation contrast provides the direct calculation in terms of the segmented out voxels of the respective objects. Thus in order to compare with the archimedian results the following formula was used to compute the fraction of matrix vis a vis the open porosity :

$$\gamma = \frac{OP.vox}{Mat.vox+Op.vox} \quad (1)$$

Where γ = volume fraction of open porosity, Op.vox = open porosity voxels, Mat. Vox = matrix voxels.

From the above equation the fraction of open porosity has been computed as 38%. The corresponding green density of the compact before the SHS step was about 40%. Previous reports provide estimates of nearly 60% porosity measured by Archimedes principle on porous NiTi sample prepared by SHS[29]. It is to be noted that the measurement of porosity using the Archimedes principle gives the total porosity as its content as a fraction of the total volume. There is no discrimination in terms of its types as open porosity or closed porosity. However it is expected that majority of the pores are of the open porosity type in SHS due to the fact that there is significant volume contraction during the formation of single phase NiTi from its constituent powders. The other sources of porosity arise from the liquid to solid contraction, the martensitic nature of transformation and gas evolution during SHS. Thus the fact that measurement of open porosity content has been only 38% using micro-tomography, is an underestimate in comparison to the expected total porosity of about 60%. As the tomography technique provides unambiguous estimation of the porosity this difference could be ascribed to the local fluctuations in porosity content and a small sample size that is of inadequate volume to contain the representative pore fraction of the sample prepared by SHS. Further it is also noticed from figure 1 that the center seems to have larger open pore content than the edge location where the sample for tomography has been extracted. Nevertheless the micro-tomography of the small sample has revealed the

morphology of open porosity and also the presence of micro-pores within the matrix. The table 1 provides the results of the overall quantitative analysis of the matrix, open pore and micro-pore content in the sample. It has been estimated from the quantitative analysis that the volume fraction of the micro-pore is about 1%.

The presence of porosity is quite important functional requirement as it not only reduces the modulus of the NiTi based implant the levels of the surrounding bone but also provides non-invasive anchoring of the implant by promoting bone in-growth. Assuming the rule of mixtures apply the following formula can be used based on the micro-tomographic quantitative evaluation to calculate the final effective modulus of the anchored NiTi implant.

$$E_{eff} = (\gamma_{Mat} - \gamma_{\mu p})E_{Mat} + \gamma_{Op}E_B \quad (2)$$

Where E_{eff} = effective modulus of bone and implant; E_{Mat} = modulus of matrix; E_B = Modulus of bone; γ_{Mat} = volume fraction of matrix ; $\gamma_{\mu p}$ = volume fraction of micro-porosity ; γ_{Op} = volume fraction open matrix porosity.

Thus considering the present volume fraction results of matrix, open porosity and micro-pore, and considering the modulus of the NiTi matrix and bone in-growth to be 40 GPa and 20 GPa respectively the effective modulus of the implant if it were integrated in the body would be about 31 GPa. On considering the open porosity content upto about 60% as is expected from archimedian results, the effective modulus would reduce to about 27 GPa. Thus if there is spatial heterogeneity in the porosity content from about 38 % to 60% the corresponding change in the spatial modulus values will be 4 GPa. Such information of the possible spatial heterogeniety in porous NiTi has not been reported earlier and is expected to be an important factor to maximise recovery strain and minimize strain incompatibilities within the implant during load excursions.

The micro-porosity seen in the matrix of the NiTi has been quantitatively analysed. The results are shown in figure 4 in terms of size and sphericity distribution, and variation of the volume as a function of the size. It is seen that the size distribution peaks at about 10µm and extends upto about 600µm. The frequency distribution beyond 40µm remains at low level. However the average volume at these large sizes almost linearly increases to levels greater than the peak levels observed below 40µm. It can be concluded from these trends that the micro-porosities in the matrix are of two types - one that has a distinct size distribution where the average volume in

each size range is maximum at the peak size frequency, a second one where occurrence is independent of the size but with increasing average volume as porosity dimensions increase. The latter type of porosity (indicated as large close porosity in the matrix) may likely be due to the intersection of the open porosity channels with matrix. Thus it can be concluded that the size of the open porosities within the scanned volume ranged from 40 to 600 µm. The smaller porosities could be due to gas evolution during the SHS. The sphericity distribution has been shown in figure 4(c). It is clearly seen that the distribution peaks at a sphericity value greater than 0.5 suggesting that the morphology of the pores tends to be in the form of oblate/prolate spheroids.

The presence of micro-pores in the matrix is of significance owing to the fact that they may reduce the fatigue properties of NiTi by being sources of fatigue cracks. The complex nature of the open porosity in the SHS fabricated NiTi is one of the important factors that lowers the modulus and also increases the anchoring of the implant by promoting bone in-growth. Thus the mechanical response implant – bone integral structure also depends on the architecture of the complex porosity. It has been attempted to devise metrics to not only describe the complex architecture of porosity but also provide indicators of its load bearing performance in the implant – bone structure. From the 3D visualization of the open porosity, it is clear that the complexity arises because of the presence of multiple pore channel with tortuous shapes and the presence of junctions between different pore channels. In a loaded implant integrated with bone tissue this complex architecture would locally redistribute the loads within the in-growth and provide protection against overloads. Thus it is useful to breakdown the complex architecture of porosity into structural elements that can redistribute the applied loads. The structural elements that conventionally form part of a load bearing frame consists of beams that are linked together in pairs or multiple beams are hinged together. In order to reduce the porosity architecture into a load bearing frame structure it is useful to construct a skeletonised idealization, from which the individual frame elements in the form of branches, links and junctions can be determined. This can be carried out using standard plug-in in the commercially available image analysis software ImageJ which works on binarised images. The procedure is briefly outlined below.

For the purpose of constructing the skeletonised idealization of the porosity architecture, a set of images was suitably binarized and then the skeletonisation program in ImageJ was applied. The porosity channels were reduced to a network of lines containing individual channel branches that

are linked and multiple branches forming node junctions. This network diagram for each of the images in the analysed set was then over-layed on the binarised image so that only lines corresponding to the open porosity could be delineated. These were then manually highlighted to show that the frame network to lie within the interconnected tubular porosity channels. This procedure was applied to a set to 100 consecutive image sequence stack at five locations from the sample top. The results are shown in figure 5 where for each range of the images from the top that were analysed, the overlayed image containing highlighted frame network that represents the skeletenoised idealization of the porosity has been displayed. From the network three architectural parameters have been calculated which are namely the number of branches, links and junctions comprising the frame network. In a physical sense the number of branches would represent the porosity channels, the links would give an idea of the tortuosity as it indicates the change in direction and the junction where number of would represent the connectivity. Thus a Connectivity – Tortuosity Index can be ascribed to the frame network in the following way :

$$\boldsymbol{CTI = exp\left(\frac{1}{\alpha}\frac{n_J}{n_J+n_L}\right)} \quad (3)$$

Where CTI = Connectivity – Tortuosity Index, n_L = number of links; n_J = number of Junctions; n_B = number of Branches; $\alpha = n_L / n_B$.

This expression for CTI is an empirical one combining the connectivity factor (defined as a fraction of the junctions given by $n_J/(n_J + n_L)$) with the tortuosity factor (defined as a fraction of the links or α). The values of the CTI computed for each case is shown in figure 5. It is seen that the CTI increases as the frame network complexity increased particularly due to the presence of a larger fraction of junctions. Considering the fact that the open porosity fraction is 38% in the scanned dataset volume, the result implies that the CTI would increase even further at internal locations of the fabricated part where at higher porosity fraction the architecture could assume more complex characteristic. As the CTI is computed from the fraction of links and junction which during the load of the integrated implant redistributes the load, it is implied that its increased value provides for a greater non-linearity of loading and unloading thus substantially affecting the super-elastic property. However, these direct structural interpretation of the CTI value needs to be verified using in-situ tests, which would be one of the directions of further research. In addition the present computation of the CTI value essentially reduces the 3D

porosity structure into 2D network using existing skeletonisation programs incorporated in freely available software such as ImageJ. These values need to be compared with the quantification of branches, links and junctions from a skeletonisation network determined from application of programs based on 3D propagative algorithms, which will be taken up in future.

Acknowledgements

CG is thankful Dr. J. K. Chakravartty, Director Materials Group and Dr Madangopal Krishnan, Head Glass and Advanced Materials Division, of Bhabha Atomic Research Centre, Mumbai, India for support during preparation of manuscript.

References

1. RA Ayers, TA Bateman, SJ Simske:" Porous NiTi as a material for bone engineering" in shape Memory Implants (eds. DL Yahia) 2000 73-88 Springer, Berlin Germany.

2. G Ryan, A Pandit, DP Apatsidis: "Fabrication methods of porous metals for use in Orthodontic applications", Bio. Mater. 2006 27, 2651 -2670.

3. JJ Klawitter, Am Weinstein:" The status of Porous materials to obtain direct skeletal attachment by tissue growth", Acta. Ortho. Belg. 1974 40 755-765.

4. M. Spector, MJ Michno, WH Smarook, GT Kwiatkowski:" A High modulus polymer for porous orthopedic implants : biomechanical compaibility of porous implants", J. Biomed. Mater. Res. 1978 12 665-677.

5. H. hahn, W. Palich:"Preliminary evaluation of porous metal surface titanium for orthopedic aplication", J. Biomed. Mater. Res. 1970 4 571-577.

6. S. Yue, R. M. Pillar, GC Weatherly:" The fatigue strength of porous coated Ti-6Al-4V implant alloy", J. Biomed. Mater Res. 1984 18 1043-1058.

7. DH KOhn, P Ducheneye:" A paranetric study of the factors affecting the fatigue strength of porous coated Ti-6Al-4V implant alloy", J. Biomed. res. 1990 24 1483-1501.

8. H Kienapfel, A Sprey, A. Wilke, P Griss:" Implant fixation by bone in-growth", J. Arthropasty 1999 14 355-368.

9. M. Spector:" Historical review of porous coated implants", J. Arthroplasty 1987 2 163-177.

10. SJ Simske, R. Sachdeva:" Cranial bone opposition and ingraowth in a porous nickel-titanium implant", J. Biomed Res 1995 29 527-533.

11. M Ungethum, W Blomer: "Technology of cementless hip endoprosthetics", Orthopade 1987 16 206-219.

12. MA Freeman, GT Railton:" Cementless fixation in endoprosthetics Orthopade 1987 16 206-219.

13. C Kröner, R. Singer:" Processing of metal foams - challenges and oppotunities", Adv. Eng. Mater. 2000 2 159-165.

14. IH Oh, N Nomura, N. Masahashi, S. Hanada:" MEchanical properties of porous titatnium compacts prepared by powder sintering" Scripta. Mater. 2003 49 1197-202.

15. M Thieme, KP Wieters, F. Berger, D Schawanweber, H Worch J Ndop et.al:" Titatnium powder sintering for preparaion of a porous functionally raded material destined for orthopedic implants", J. Mater Sci. Mater Med. 2001 12 225-231.

16. BM Silberstein, VE Gyunter:" Shape memory implants in spinal surgery", Berlin, Springer 2000.

17. SA Shabalovskyay:" On the nature of bio-comaptibility and on medical applications of Niti shpe memory alloys", Bio. Med. Mater. Eng. 1996 6 267-289.

18. G. Airol;di, G. Riva:" Innovative materials : The NiTi alloys in orthodontics", 1996 Biomed Mater Eng. 1996 6 299-305.

19. H. Fischer, B Vogel, A Welle:" Applications of shape memory alloys in medical instruments ", Min. inv. therapy. allied Technol. 2004 13 248-253.

20. VI Itin, VE Gyunter, SA Shabalovskya, RL Sachdeva:" Mechanical properties and shape memory of porous nitinol", Mater. Charact. 1994 32 179-187.

21. AJ Neurohr, DC Dunand:" Shape memory NoTi with two - dimesional metwork of microchannels", Acta. Biomat. 2011 7 1862-1872.

22. K Otsuka, X Ren:" Physical metallurgy of Ni-Ti based shaped memory qalloys", Prog. Metr. Sci. 2005 50 511-580.

23. BY Li, LJ Rong, Y. Li, VE Gjunter:" A recent development in producing porous NiTi shape memory alloys:" Intermetallics 2000 8 881-884.

24. BY Li, LJ Rong, Y. Li, VE Gjunter:" Synthesis of porous Ni-Ti shape memory alloys by self propagating high temperature synthesis : Reaction, MEchanism, and anisotroy of pore structure", Acta. Mater. 2000 48 3895-39904.

25. A Bansiddhi, TD Sargent, SI stupp, DC Dunand:" Porous NiTi for bobe implants: A review", Acta. Biomater. 2008 4 773-782.

26. A. Biswas : "Porous NiTi by thermal explosion mode of SHS : Processing mechanism and generation of single phase stuctures ", Acta. Mater. 2005 53 1415-1425.

27. SR Stock:" Recent advances in X-ray microtomography applied to materials ", Inter. Mater. Rev. 2008 53 129-181.

28. E. Maire, P. J. Withers: " Quantitative Tomography", Inter. Mater. Rev. 2014 59 1-43.

29. SK Roy, A. Biswas :" Combustion of powder mixtures forming reaction products - synthesis of NiAl", Min Pro Ext. Met. Rev. 2001 22 567-580.

30. SK Roy, A. Biswas :" Combustion synthesis of TiB and TiB_2 under vacuum", J. Mater. Sci. Lett. 1994 13 371- 375.

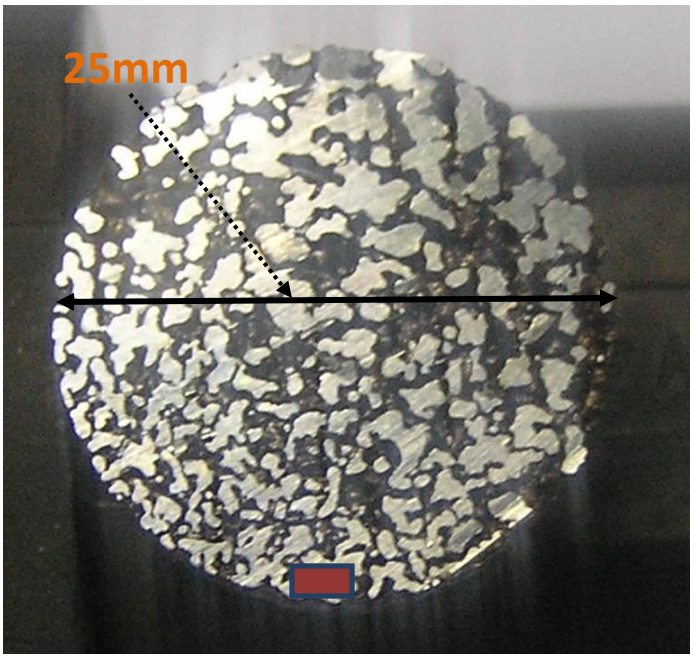

Figure 1.NiTi cylinder fabricated from SHS in the explosive mode. The colored region denotes the location of the sample extracted for the tomography scanning.

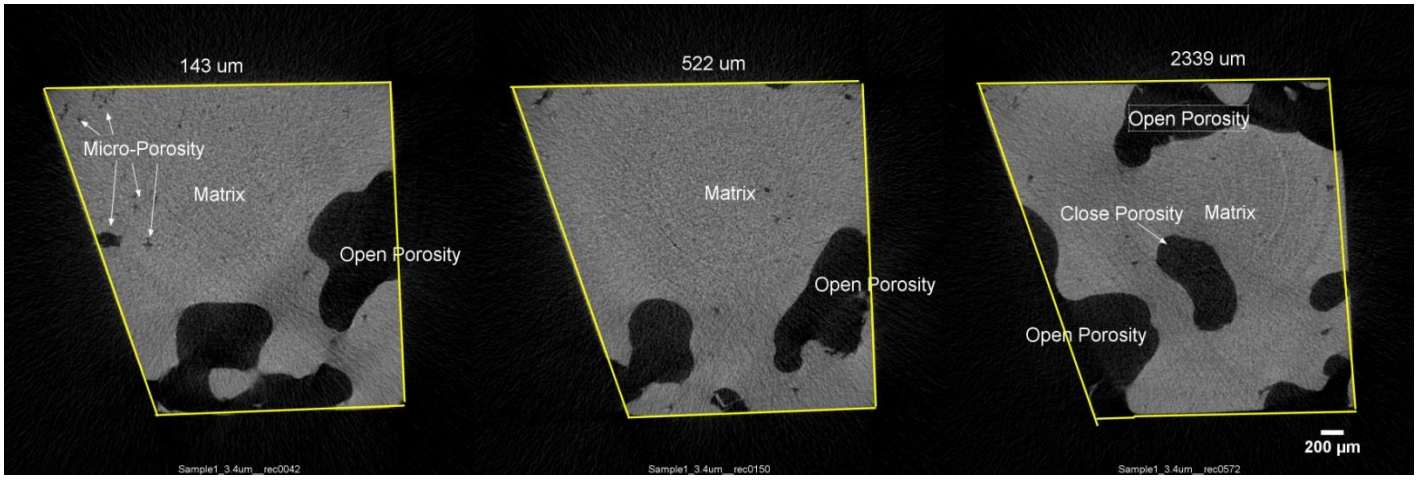

(a)

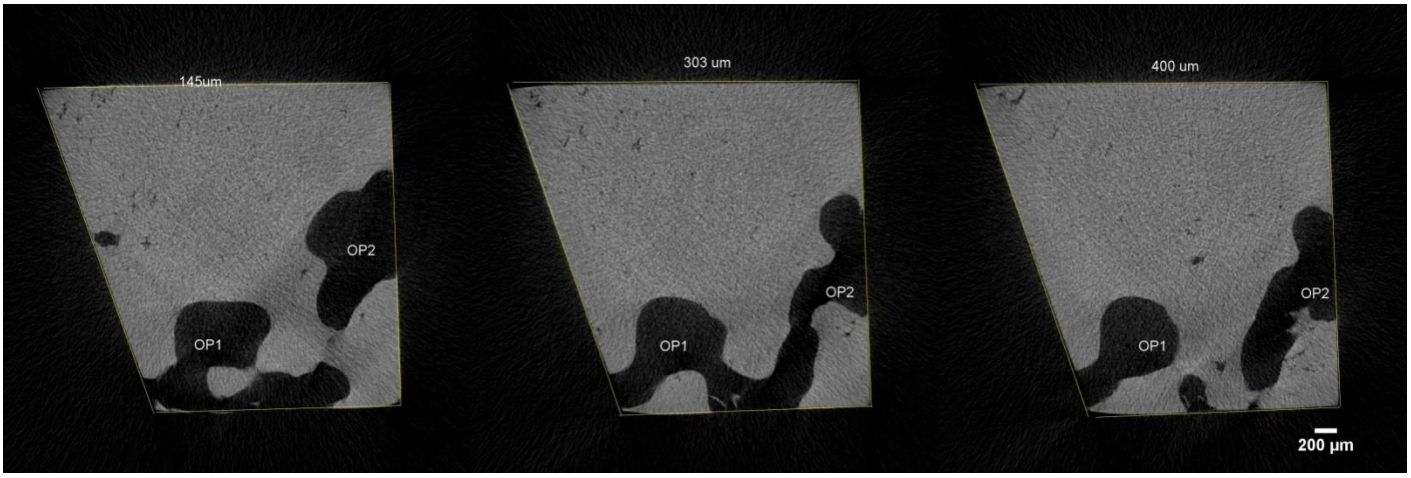

(b)

Figure 2. (a) Montage showing the types of porosity in the reconstructed image slices as a function of height from the top of the microtomography scan. (b) A montage of three images showing an example of the interconnectivity of the open porosity in the sample while traversing the image slice set across the Z axis (or sample height).

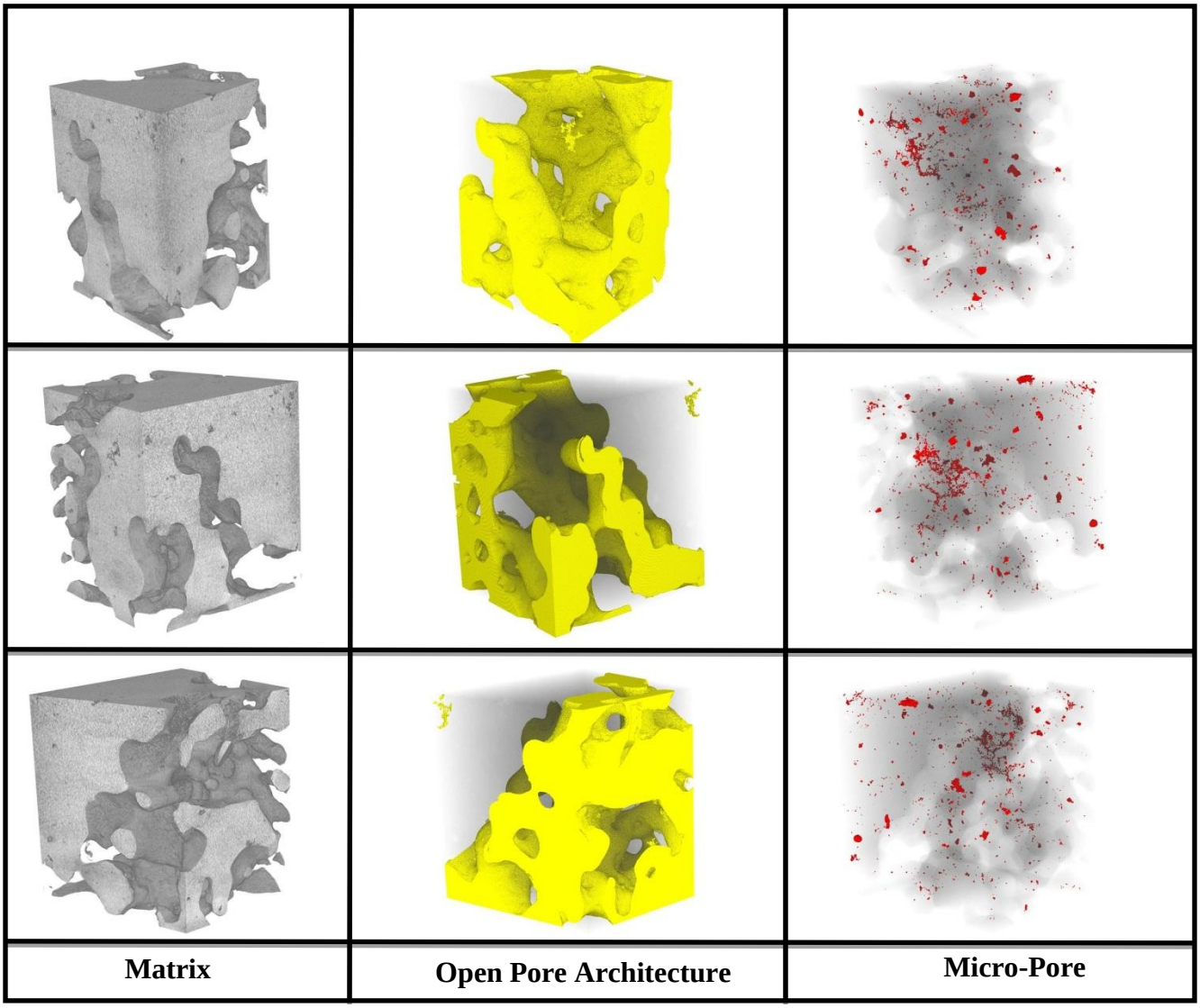

Figure 3. Perspective views at angles of 0°(top row), 90°(middle row) and 180° (bottom row) the dataset (2.9 x 2.45 x 3.54 mm^3) segmenting out the matrix, open porosity and micro-pore shown by grey, yellow and red colors respectively.

Table 1: Table showing the overall quantification analysis of the dataset

3D Quantitative parameter	Matrix	Porosity	
		Open	Micro-pore
Volume fraction (%)	61.8	38.2	1.06
Number density (10^{-3} mm^3)	-	-	57.6

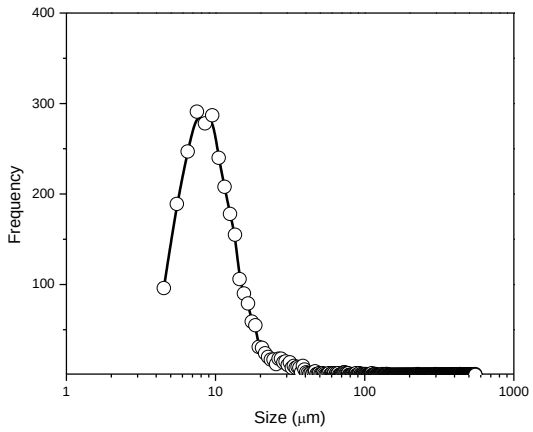

(a)

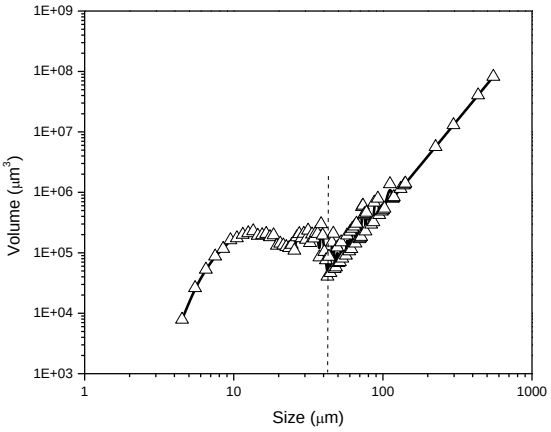

(b)

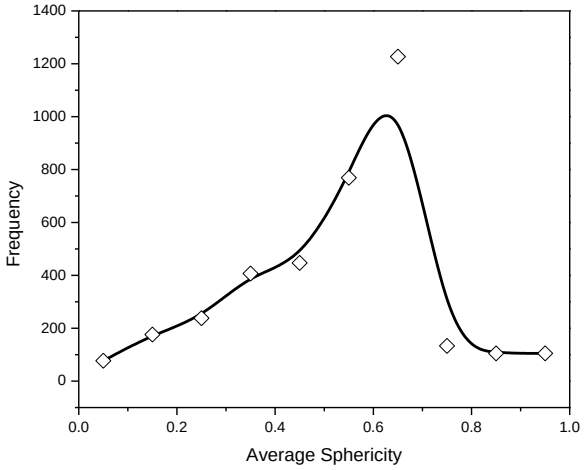

(c)

Figure 4. Quantitative analysis of the pores in the matrix (excluding the open porosity) in terms of (a) size distribution (b) volume distribution as a function of size range (c) sphericity distribution.

Sample Height Range (μm)	Skeletonised idealization of open porosity	Architectural parameters			CTI
		Branch	Link	Junction	
148 - 490	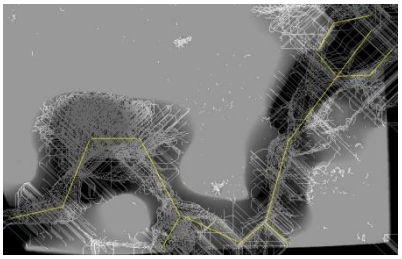	15	8	3	1.66
841 – 1186	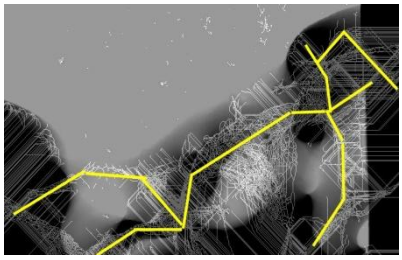	16	9	2	1.38
1538 – 1883	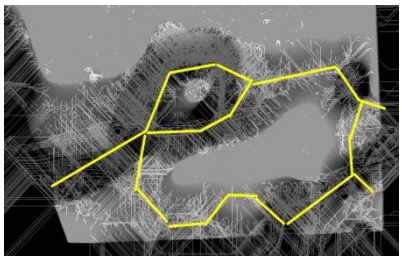	21	12	4	1.54
2293 – 2580	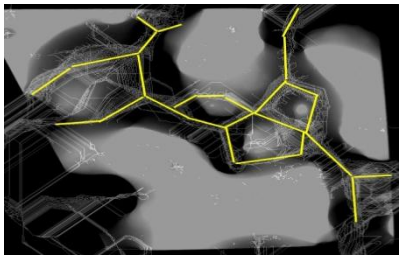	25	8	9	5.23
2935 – 3280	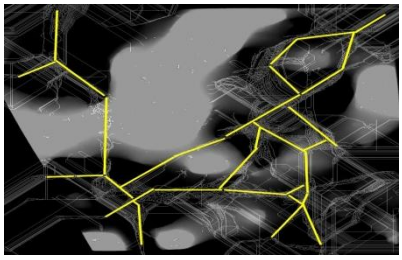	30	8	11	8.76

Figure 5. A table format depicting the nature of the skeletonised idealisation of the interconnected porosity and its quantification in terms of elements such as Branch, Links and Junctions as a function of distinct ranges of sample height from the top of the scan. The calculation of the CTI parameter based on the expression (3) is also shown.